Research Article

Influence of Drying Temperature on the Structural, Optical, and Electrical Properties of Layer-by-Layer ZnO Nanoparticles Seeded Catalyst

S. S. Shariffudin,[1] M. H. Mamat,[1] S. H. Herman,[1] and M. Rusop[1, 2]

[1] *NANO-ElecTronic Centre, Faculty of Electrical Engineering, Universiti Teknologi MARA, Selangor, 40450 Shah Alam, Malaysia*
[2] *NANO-SciTech Centre, Institute of Science, Universiti Teknologi MARA, Selangor, 40450 Shah Alam, Malaysia*

Correspondence should be addressed to S. S. Shariffudin, sobihana@gmail.com

Layer-by-layer zinc oxide (ZnO) nanoparticles have been prepared using sol-gel spin coating technique. The films were dried at different temperature from 100°C to 300°C to study its effect to the surface morphology, optical and electrical properties of the films. Film dried at 200°C shows the highest (0 0 2) peak of X-ray diffraction pattern which is due to complete decomposition of zinc acetate and complete vaporization of the stabilizer and solvent. It was found that the grain size increased with the increased of drying temperature from 100 to 200°C, but for films dried at above 200°C, the grain size decreased. Photoluminescence measurements show a sharp ultraviolet emission centred at 380 nm and a very low intensity visible emission. Blue visible emission was detected for sample dried at temperature below 200°C, while for films dried above 250°C, the visible emission is red shifted. The films were transparent in the visible range from 400 to 800 nm with average transmittance of above 85%. Linear *I-V* characteristics were shown confirming the ohmic behaviour of the gold contacts to the films. A minimum resistivity was given by 5.08 $\Omega \cdot$ cm for the film dried at 300°C.

1. Introduction

Recently, ZnO is aggressively used in optoelectronic devices such as light emitting diodes and solar cells due to its properties of direct band gap of 3.37 eV and high exciton binding energy of 60 meV. Nanorods, nanowires, nanoflowers, nanoparticles, nanowalls, and nanotubes were among the many kinds of ZnO nanostructures that have been produced by many. In order to grow ZnO nanorods and nanowires, various methods have been applied such as chemical vapour deposition (CVD) method [1], metal organic CVD (MOCVD) [2], aqueous chemical growth (ACG) method [3], and spray pyrolysis [4].

In the CVD method, vapour-liquid-solid (VLS) mechanism had been applied since quite some time ago, which uses metals such as gold [5] and platinum [6], or transition metal such as nickel [7] as the catalyst to enhance the growth of the ZnO nanorods. However, due to the impurity of the metal to the ZnO nanorods, researches started to employ noncatalyst or self-catalysed process, which applied vapour-solid (VS) mechanism as the growth method. According to Cha et al., the growth direction of the ZnO nanowires depended on the crystal structure of the substrate or seeded catalyst [8]. In order for the ZnO nanorods to grow vertically aligned with good quality, the ZnO seeded catalyst needs to be highly (0 0 2) hexagonal orientation [9]. However until date, there is no report on the growth of ZnO nanorods using seeded catalyst deposited using sol-gel spin coating technique. Sol-gel spin coating technique has been widely used to deposit thin films due to its ease of deposition, homogeneity, and low crystallization temperature [10]. Furthermore, many have reported on producing highly c-axis ZnO thin films using spin coating technique either single crystal [11, 12] or polycrystalline [10, 13, 14]. Therefore the aim of our study is to deposit ZnO nanoparticles using spin coating technique with high c-axis orientation to be used as seeded catalyst for the growth of ZnO nanorods by CVD method.

In the present work, we studied the physical properties, photoluminescence spectra, transmittance spectra, and current-voltage (*I-V*) characteristics of the sol-gel spin coated ZnO thin films in order to investigate the optimum properties of the ZnO nanoparticles to be used as seeded catalyst.

2. Experimental Procedure

Zinc acetate dihydrate ($Zn(CH_3COO)_2 \cdot 2H_2O$, 99%; Sigma-Aldrich) was dissolved in 2-methoxyethanol ($C_3H_8O_2$, 99%; Sigma-Aldrich) with addition of monoethanolamine (MEA: $H_2NCH_2CH_2OH$, 99.5%; Merck) as the stabilizer. The concentration of zinc acetate was 0.4 mol/L while the molar ratio of MEA to zinc acetate was kept at 1.0. The solution was stirred on a hot plat stirrer with applied temperature of 80°C for 1 hour to produce a homogenous solution. It is then aged for 24 hours before the spincoating was done. Quartz substrates were cleaned using acetone, methanol, and deionized water in ultrasonic for 10 minutes, respectively. The solutions were dropped onto the spinning substrates with a rotation speed of 3000 rpm for 30 s. The films were then dried at different temperature (100°C, 150°C, 200°C, 250°C, and 300°C) for 10 minutes in furnace to evaporate the solvents and remove organic residuals, followed by annealing in air at 500°C for 1 h. This process of coating-drying-annealing was repeated for four times until the desired thickness of the films was obtained.

The thickness of the ZnO nanostructures was measured using surface profiler (model: Veeco Dektak 750). The crystalline phase of the ZnO nanostructures was determined by X-Ray diffractometer (XRD; model: Rigaku Ultima). The surface morphology of the films were checked using field emission scanning electron microscopy (FE-SEM; model: JEOL JSM-7600F) with accelerating voltage of 5 kV. For optical characteristics, photoluminescence (PL) spectrometer (model: Horiba Jabin Yvon) using the 325 nm He-Cd laser as the excitation source to measure the photoluminescence spectra, and UV-Vis/NIR spectrophotometer (model: JASCO V-670) to characterize the optical transmittance spectra. Meanwhile for electrical measurements, gold was firstly sputtered on the films with a thickness of about 60 nm as the metal contact. 2-point probe (model: Advantest 6234) was used for the *I-V* measurement.

3. Results and Discussion

3.1. Physical Properties. We first present the XRD patterns of the ZnO nanoparticles films dried at temperature of 100°C to 300°C in Figure 1. The XRD patterns clearly show that all films are in good agreement with standard ZnO diffraction pattern (JCPDS no 36-1451). It is observed that diffraction peaks 2θ of 31.95°, 34.6°, and 36.35° which correspond to (1 0 0), (0 0 2), and (1 0 1) crystalline structure appeared at all films, and for the case of film dried at 100°C, all the intensities are nearly the same. When the drying temperature was increased to 150°C, the (0 0 2) intensity increases while the (1 0 0) and (1 0 1) intensities decrease. The (0 0 2) peak becomes dominant and reaches the maximum intensity for
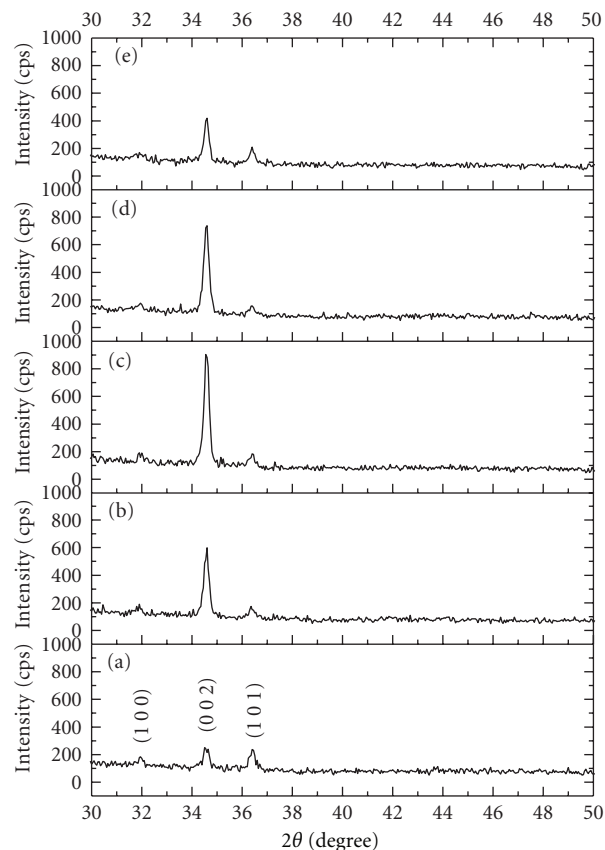

Figure 1: XRD patterns of the ZnO thin films at drying temperature of (a) 100°C, (b) 150°C, (c) 200°C, (d) 250°C, and (e) 300°C.

film dried at 200°C. When the temperature was increased to more than 200°C, the intensity of the (0 0 2) peak started to decrease until drying temperature reached 300°C. According to Xu et al., the c-axis growth of sol-gel ZnO films is originated from intrinsic and extrinsic factors [15]. For the intrinsic factor, (0 0 2) orientation is thermodynamically favourable growth direction due to its minimum surface free energy [16]. The conditions during the thin films preparations become the extrinsic factor of the c-axis orientation, which for the case of sol-gel method is highly dependent on the type of stabilizer used in the solution preparation. For our case, it is a combination of intrinsic and extrinsic factors, and also with the help of self-template of the layer-by-layer process. The growth mechanism is as follows. The first layer was spin coated onto substrate and was randomly oriented. When the layer is dried, the stabilizer and solution vapoured, and this was followed by annealing which makes the film crystallized at (0 0 2) due to the minimum surface energy. Then when the second layer was spin coated, the first layer becomes a template to the next layer which helps the orientation to become more c-axis. With sufficient number of layers, the (0 0 2) orientation becomes most dominant compared to the other weak peaks.

Contemplating from the phenomenon, we deduce that the temperature during the drying process affects the crystallization of the ZnO as follows. The boiling temperature for
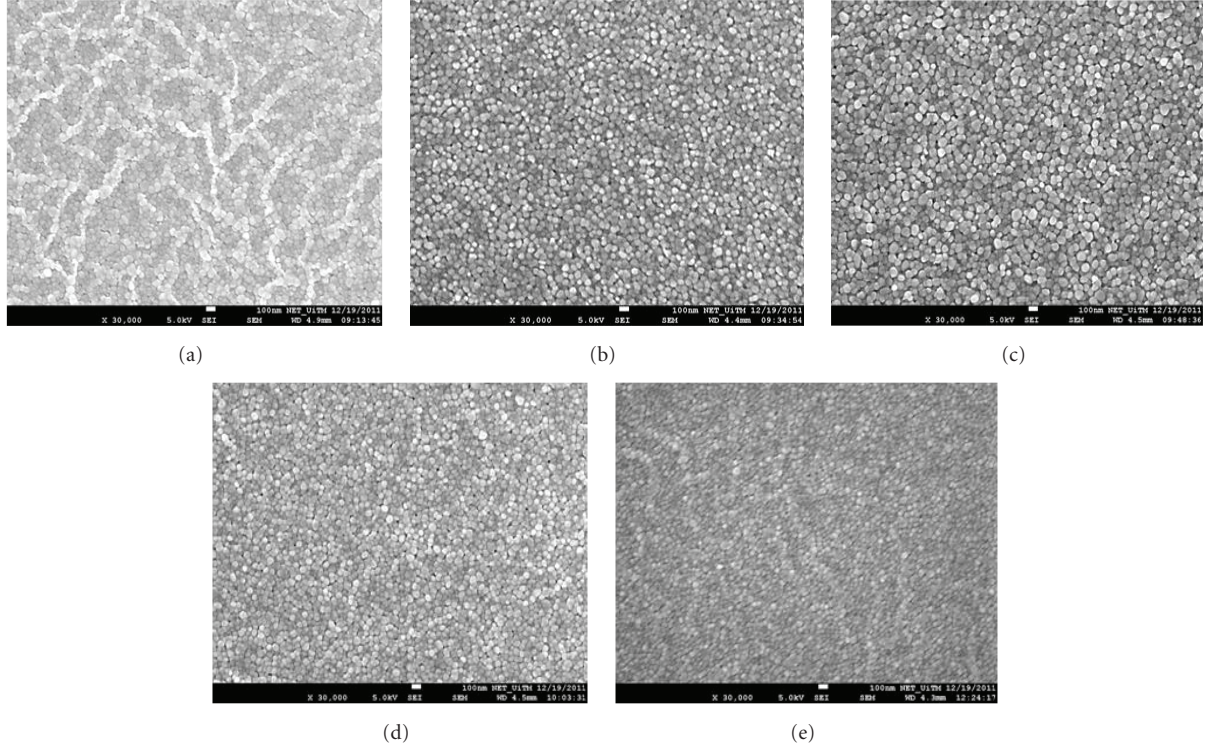
(a)

(b)

(c)

(d)

(e)

FIGURE 2: FE-SEM micrographs of the sol-gel layer-by-layer ZnO thin films dried at (a) 100°C, (b) 150°C, (c) 200°C, (d) 250°C, and (e) 300°C.

MEA is about 170°C, so a minimum temperature of 170°C is required to vapour the stabilizer from the thin films during the drying process. If the temperature is lower than that, the vaporization of the solvent and stabilizer and also thermal decomposition of the zinc acetate are not complete during the drying process. This causes abrupt vaporization of the solvent during the annealing process, which will affect the crystallization of the ZnO [17]. However when the drying temperature is increased to above 240°C, the temperature is too high which also causes the solvent to vapour abruptly during the drying process.

The grain size of the ZnO can be calculated from the XRD pattern, using Scherer's formula [18] as depicted in (1) below:

$$D = \frac{0.9\lambda}{\beta \cos\theta},\qquad(1)$$

where D is the mean size of the ZnO particles, λ is the X-ray wavelength, β is the full width of half maximum of (0 0 2) peak for ZnO, and θ is the maximum angle of the (0 0 2) peak in radians. The calculated grain sizes are tabulated in Table 1. It is observed that the grain size increased from 37.1 nm to 41.6 nm when the temperature increased to 200°C. For films dried at temperature above 250°C, the grain size decreased from 36.3 nm to 36.0 nm. According to Kim et al. [19], when the film is dried at temperature of below 250°C, the particle size may increased due to nondisturbance of the preferential growth during the annealing process. For the films dried

TABLE 1: Average particles size for ZnO nanoparticles at different drying temperature.

Drying temperature (°C)	Average grain size (nm)	Film thickness (nm)
100	37.1	109.5
150	37.9	93.9
200	41.6	90.5
250	36.3	104.8
300	36.0	110.2

above 250°C, the abrupt vaporization of the solvents disturbed the crystal growth, thus decreases the particle size.

Figure 2 shows the FE-SEM micrographs of the ZnO films dried at different temperatures. The micrographs show that the ZnO nanoparticles films are porous, which is a common phenomenon for sol-gel ZnO thin films [20, 21]. The grains become more uniform and denser as the drying temperature increases from 100 to 200°C.

3.2. Optical Properties. Room temperature PL spectra were measured in the wavelength range of 350 to 700 nm. Figure 3 shows the PL spectra for the ZnO nanoparticles films dried at different temperature. From the PL spectra, three peaks were detected, UV emission peak centered at 380 nm, visible peak centered at about 440 nm, and another peak centered at 580 nm. The UV emission is attributed to the free-exciton emission [22, 23]. It is observed that the intensity of the UV
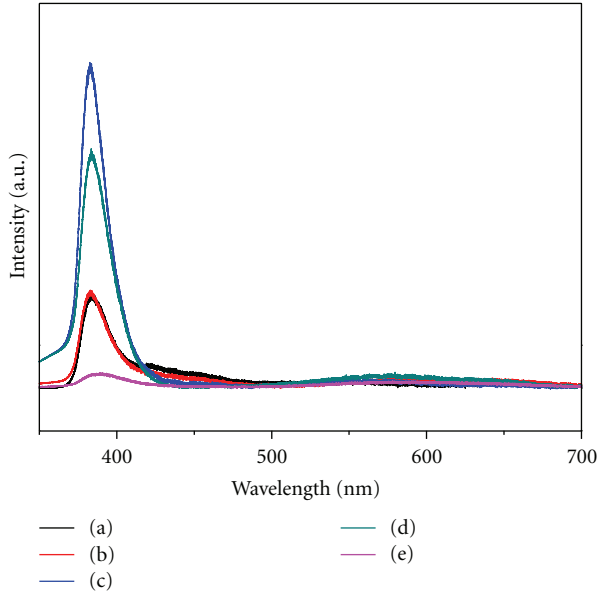
FIGURE 3: Photoluminescence spectra of the ZnO nanoparticles dried at (a) 100°C, (b) 150°C, (c) 200°C, (d) 250°C, and (e) 300°C.

FIGURE 4: Comparison of PL spectra of ZnO nanoparticles dried at 100°C and 150°C.

emission gradually increased with the drying temperature. However, when the temperature was increased above 200°C, the intensity decreased. It is known that the UV emission is related to the crystalline structure of the ZnO films as described by Xu et al. [15] and Chatterjee et al. [24]. When the crystalline quality is improved, the density of the free exciton becomes higher, which is correlated to the UV emission. It is also found that the UV emission is also affected by the grain size of the ZnO [24] which is in great agreement with the XRD result.

It is known that visible emission of PL in ZnO is attributed to crystalline defect such as Zn interstitial and oxygen vacancy. According to Schmit-Mende, the intrinsic defects are known as $Zn_i^{\blacklozenge\blacklozenge}, Zn_i^{\blacklozenge}, Zn_i^{X}, V_O^{\blacklozenge\blacklozenge}, V_O^{\blacklozenge}$, and V_O which are the donor defects; V_{Zn}'' and V_{Zn}' which are the acceptor defects [25]. Until now the dominant defect of the visible emission is still a controversy, but either V_O or Zn_i is generally considered as the primary defect responsible for this emission [26]. ZnO films dried at 100°C and 150°C show a shoulder peak of blue emission centred at 440 nm as depicted in Figure 4. The blue emission is originated from the electron transition from the shallow donor level of oxygen vacancies to the valence band [27]. However, for the films dried at above 250°C, visible emission is red shifted to broad emission centred at about 570 nm as shown in Figure 5. When the temperature was further increased to 300°C, the intensity becomes quenched and more red shifted. According to O'Brien et al. the yellow-orange emission is attributed to the interstitial oxygen ions [28].

From the PL spectra, band gap of the ZnO can be calculated using Planck's constant as in (2):
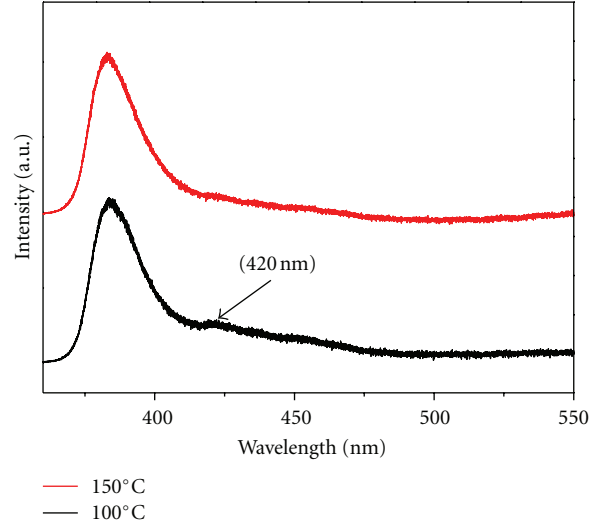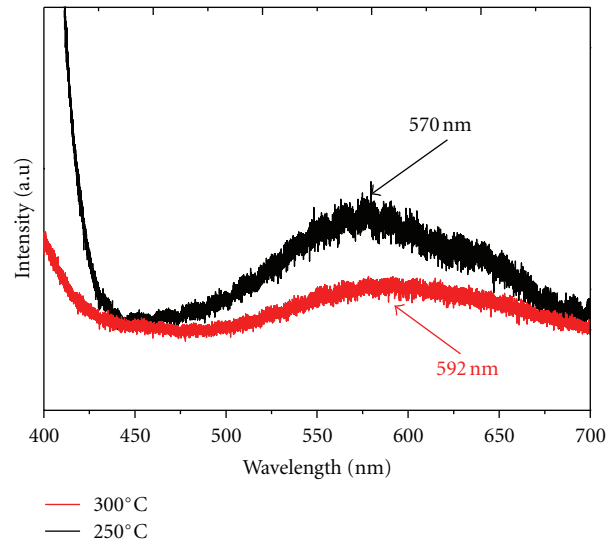
$$E = \frac{hc}{\lambda}, \tag{2}$$

FIGURE 5: Comparison of PL spectra of ZnO nanoparticles dried at 250°C and 300°C.

where E is the the band gap, h is the Planck's constant with a value of 4.135667×10^{-15} eVs, c is the velocity of light of 3.0×10^8, and λ is the wavelength of the spectra in the UV emission. Optical band gaps of the ZnO nanoparticles are shown in Table 2. It was found that the band gap increases with the drying temperature and maximized at temperature of 200°C; when the temperature is increased to more than 250°C, the optical band gap decreases with lowest value given by films dried at 300°C. It is found that the optical band gap is influenced by the crystalline quality of the films.

Transmittance spectra were measured within the wavelength of 300 to 700 nm and are shown in Figure 6. The sharp ultraviolet absorption edges at the wavelength of about 370 nm. The average transmittance spectra in the visible emission increased with the drying temperature but

TABLE 2: Optical band gap and average transmittance of the ZnO nanoparticles at different drying temperatures.

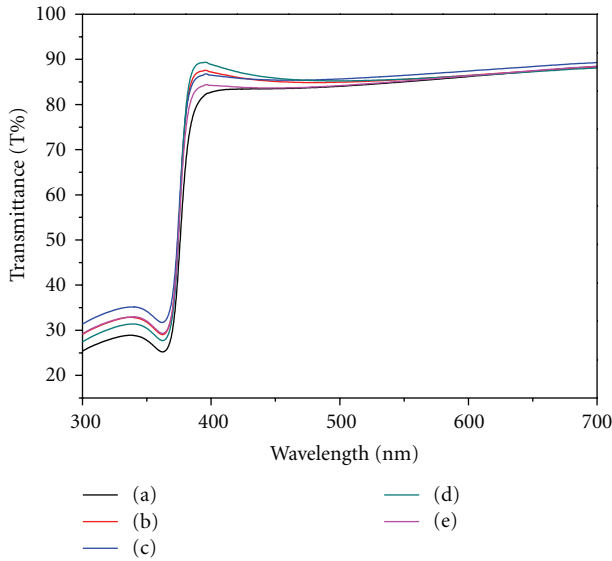| Drying temperature	100°C	150°C	200°C	250°C	300°C
Optical band gap (eV)	3.23	3.24	3.25	3.23	3.20
Average transmittance (%)	85.32	86.15	86.84	86.40	85.52

FIGURE 6: Transmittance spectra of the ZnO nanoparticles dried at (a) 100°C, (b) 150°C, (c) 200°C, (d) 250°C, and (e) 300°C.

decreased when the temperature reached 250°C and above as shown in Table 2. Contemplating from the phenomena, we deduce that the transparency of the films is dependent on the crystalline quality. The transmittance is lower in lower c-axis sample because much light is dispersed in the grain boundary [19]. Highest transparency is given by film dried at 200°C which is 86.84%, which also shows the highest c-axis orientation.

3.3. Electrical Properties. *I-V* measurements were done in room temperature with applied voltage in the range of −10 V to 10 V. Linear *I-V* curves are shown in Figure 7(a), indicating that all of the ZnO nanoparticles show ohmic behaviour with the gold metal contact. It is observed that the current increased with the drying temperature, with the highest current given by film dried at 300°C. From the *I-V* graph, resistivity was calculated and shown in Figure 7(b). As expected from the current value, the resistivity is inversely proportionate to the drying temperature. For the case of films annealed at temperature lower than 200°C, the resistivity decrease with the increasing temperature might be due to the improvement of the crystalline quality and also the increase of grain size [29]. When the drying temperature was further increased to 250°C, the resistivity keeps on decreasing even though the crystalline structure was decreased. The cause to this phenomenon is still under our investigation.
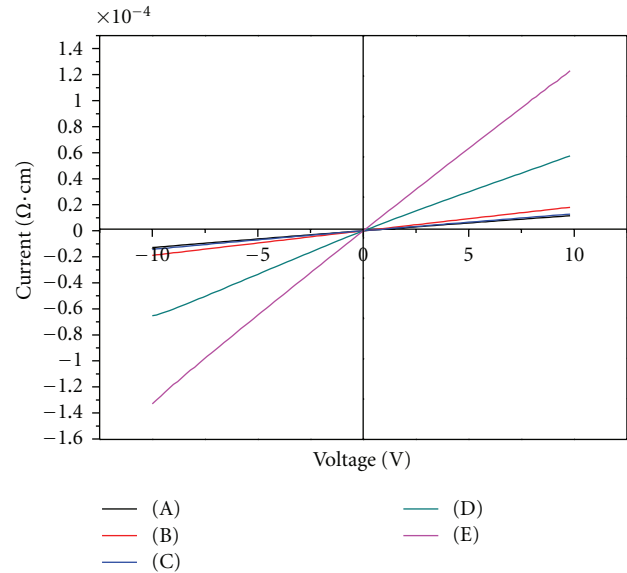
(a)
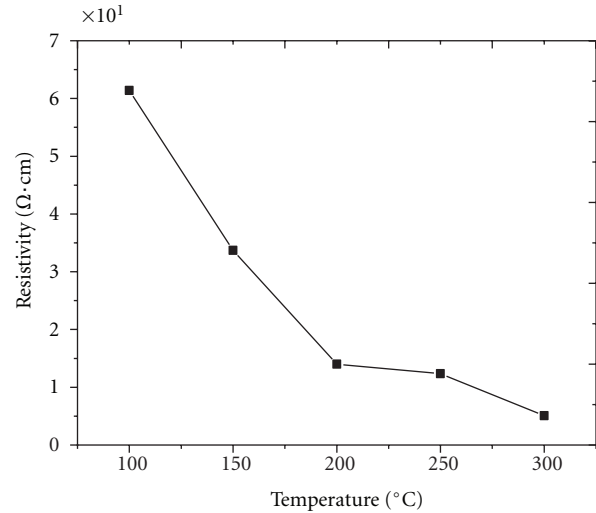
(b)

FIGURE 7: (a) *I-V* measurements of the sol-gel layer-by-layer ZnO thin films dried at (A) 100°C, (B) 150°C, (C) 200°C, (D) 250°C, and (E) 300°C and (b) resistivity of the ZnO nanoparticles at different drying temperature.

4. Conclusion

ZnO nanoparticles films were deposited using sol-gel spin coating technique on quartz substrates to be used as seeded catalyst. It was found that the crystalline structure, morphology, optical, and electrical properties were highly

dependent on the drying temperature. We conclude that the optimum drying temperature for the ZnO films to be used as seeded catalyst was at 200°C, which showed highest (0 0 2) diffraction peak due to complete vaporization of the solvent and decomposition of the zinc acetate. Morphologies were also affected by the drying temperature, with the grain size increasing with the drying temperature until 200°C. PL spectra indicated that the film dried at 200°C exhibits the highest UV emission peak which is due to the highest crystalline structure. Resistivity of the films decreased with the temperature due to the improvement of the crystalline quality up to 200°C.

Acknowledgments

References

[1] C. Wongchoosuk, K. Subannajui, A. Menzel et al., "Controlled synthesis of ZnO nanostructures: the role of source and substrate temperatures," *The Journal of Physical Chemistry C*, vol. 115, no. 3, pp. 757–761, 2011.

[2] K. S. Kim and H. W. Kim, "Synthesis of ZnO nanorod on bare Si substrate using metal organic chemical vapor deposition," *Physica B*, vol. 328, no. 3-4, pp. 368–371, 2003.

[3] X. Liu, Z. Jin, S. Bu, J. Zhao, and K. Yu, "Preparation of ZnO nanorods and special lath-like crystals by aqueous chemical growth (ACG) method," *Materials Science and Engineering B*, vol. 129, no. 1–3, pp. 139–143, 2006.

[4] T. Dedova, M. Krunks, M. Grossberg, O. Volobujeva, and I. Oja Acik, "A novel deposition method to grow ZnO nanorods: spray pyrolysis," *Superlattices and Microstructures*, vol. 42, no. 1–6, pp. 444–450, 2007.

[5] S. Y. Pung, K. L. Choy, and X. Hou, "Tip-growth mode and base-growth mode of Au-catalyzed zinc oxide nanowires using chemical vapor deposition technique," *Journal of Crystal Growth*, vol. 312, no. 14, pp. 2049–2055, 2010.

[6] C. Andreazza-Vignolle, P. Andreazza, and D. Zhao, "Catalyst effect on ZnO nanostructure shape," *Superlattices and Microstructures*, vol. 39, no. 1–4, pp. 340–347, 2006.

[7] S. C. Lyu, Y. Zhang, H. Ruh et al., "Low temperature growth and photoluminescence of well-aligned zinc oxide nanowires," *Chemical Physics Letters*, vol. 363, no. 1-2, pp. 134–138, 2002.

[8] S. N. Cha, B. G. Song, J. E. Jang et al., "Controlled growth of vertically aligned ZnO nanowires with different crystal orientation of the ZnO seed layer," *Nanotechnology*, vol. 19, no. 23, Article ID 235601, 2008.

[9] C. Li, G. Fang, J. Li, L. Ai, B. Dong, and X. Zhao, "Effect of seed layer on structural properties of ZnO nanorod arrays grown by vapor-phase transport," *The Journal of Physical Chemistry C*, vol. 112, no. 4, pp. 990–995, 2008.

[10] M. Caglar, S. Ilican, Y. Caglar, and F. Yakuphanoglu, "Electrical conductivity and optical properties of ZnO nanostructured thin film," *Applied Surface Science*, vol. 255, no. 8, pp. 4491–4496, 2009.

[11] Y. Natsume and H. Sakata, "Zinc oxide films prepared by sol-gel spin-coating," *Thin Solid Films*, vol. 372, no. 1, pp. 30–36, 2000.

[12] Y. S. Ho and K. Y. Lee, "Fabrication of highly oriented (002) ZnO film on glass by sol-gel method," *Thin Solid Films*, vol. 519, no. 4, pp. 1431–1434, 2010.

[13] M. Saleem, L. Fang, H. Ruan et al., "Effect of zinc acetate concentration on the structural and optical properties of ZnO thin films deposited by Sol-Gel method," *International Journal of Physical Sciences*, vol. 7, no. 23, pp. 2971–2979, 2012.

[14] J. Sengupta, R. K. Sahoo, K. K. Bardhan, and C. D. Mukherjee, "Influence of annealing temperature on the structural, topographical and optical properties of sol-gel derived ZnO thin films," *Materials Letters*, vol. 65, no. 17-18, pp. 2572–2574, 2011.

[15] L. Xu, X. Li, Y. Chen, and F. Xu, "Structural and optical properties of ZnO thin films prepared by sol-gel method with different thickness," *Applied Surface Science*, vol. 257, no. 9, pp. 4031–4037, 2011.

[16] N. Fujimura, T. Nishihara, S. Goto, J. Xu, and T. Ito, "Control of preferred orientation for ZnOx films: control of self-texture," *Journal of Crystal Growth*, vol. 130, no. 1-2, pp. 269–279, 1993.

[17] A. Pakdel and F. E. Ghodsi, "Influence of drying conditions on the optical and structural properties of sol-gel-derived ZnO nanocrystalline films," *Pramana*, vol. 76, no. 6, pp. 973–983, 2011.

[18] A. K. Singh, V. Viswanath, and V. C. Janu, "Synthesis, effect of capping agents, structural, optical and photoluminescence properties of ZnO nanoparticles," *Journal of Luminescence*, vol. 129, no. 8, pp. 874–878, 2009.

[19] Y. S. Kim, W. P. Tai, and S. J. Shu, "Effect of preheating temperature on structural and optical properties of ZnO thin films by sol-gel process," *Thin Solid Films*, vol. 491, no. 1-2, pp. 153–160, 2005.

[20] A. R. Bari, M. D. Shinde, V. Deo, and L. A. Patil, "Effect of solvents on the particle morphology of nanostructured ZnO," *Indian Journal of Pure and Applied Physics*, vol. 47, no. 1, pp. 24–27, 2009.

[21] N. J. Kim, S. L. Choi, H. J. Lee, and K. J. Kim, "Nanostructures and luminescence properties of porous ZnO thin films prepared by sol-gel process," *Current Applied Physics*, vol. 9, no. 3, pp. 643–646, 2009.

[22] K. F. Lin, H. M. Cheng, H. C. Hsu, L. J. Lin, and W. F. Hsieh, "Band gap variation of size-controlled ZnO quantum dots synthesized by sol-gel method," *Chemical Physics Letters*, vol. 409, no. 4–6, pp. 208–211, 2005.

[23] Q. Li, J. Bian, J. Sun et al., "Controllable growth of well-aligned ZnO nanorod arrays by low-temperature wet chemical bath deposition method," *Applied Surface Science*, vol. 256, no. 6, pp. 1698–1702, 2010.

[24] A. Chatterjee, C. H. Shen, A. Ganguly et al., "Strong room-temperature UV emission of nanocrystalline ZnO films derived from a polymeric solution," *Chemical Physics Letters*, vol. 391, no. 4–6, pp. 278–282, 2004.

[25] L. Schmidt-Mende and J. L. MacManus-Driscoll, "ZnO—nanostructures, defects, and devices," *Materials Today*, vol. 10, no. 5, pp. 40–48, 2007.

[26] P. Sagar, P. K. Shishodia, R. M. Mehra, H. Okada, A. Wakahara, and A. Yoshida, "Photoluminescence and absorption in sol-gel-derived ZnO films," *Journal of Luminescence*, vol. 126, no. 2, pp. 800–806, 2007.

[27] D. H. Zhang, Z. Y. Xue, and Q. P. Wang, "The mechanisms of blue emission from ZnO films deposited on glass substrate by r.f. magnetron sputtering," *Journal of Physics D*, vol. 35, no. 21, pp. 2837–2840, 2002.

[28] S. O'Brien, L. H. K. Koh, and G. M. Crean, "ZnO thin films prepared by a single step sol-gel process," *Thin Solid Films*, vol. 516, no. 7, pp. 1391–1395, 2008.

[29] J. H. Lee, K. H. Ko, and B. O. Park, "Electrical and optical properties of ZnO transparent conducting films by the sol-gel method," *Journal of Crystal Growth*, vol. 247, no. 1-2, pp. 119–125, 2003.

Journal of
Nanotechnology

International Journal of
Corrosion

International Journal of
Polymer Science

**Smart Materials
Research**

Journal of
Composites

**BioMed
Research International**

Journal of
Metallurgy

Journal of
Materials

Hindawi

Submit your manuscripts at
http://www.hindawi.com

Journal of
Nanoparticles

Advances in
Materials Science and Engineering

Scientifica

Journal of
Nanomaterials

**The Scientific
World Journal**

International Journal of
Biomaterials

Journal of
Nanoscience

Journal of
Coatings

Journal of
Crystallography

Journal of
Ceramics

Journal of
Textiles